J. Chem. Sci. Vol. 128, No. 6, June 2016, pp. 957–965. © Indian Academy of Sciences.
DOI 10.1007/s12039-016-1094-0

Direct synthesis of dimethyl carbonate from CO_2 and methanol over CeO_2 catalysts of different morphologies

UNNIKRISHNAN P[a,b] and SRINIVAS DARBHA[a,b,*]

[a]Catalysis and Inorganic Chemistry Division, CSIR-National Chemical Laboratory, Dr. Homi Bhabha Road, Pune 411 008, India
[b]Academy of Scientific and Innovative Research (AcSIR), New Delhi, India
e-mail: d.srinivas@ncl.res.in

MS received 4 January 2016; revised 11 April 2016; accepted 11 April 2016

Abstract. The direct synthesis of dimethyl carbonate (DMC) from carbon dioxide (CO_2) and methanol is an attractive approach towards conversion of the greenhouse gas - CO_2 into value-added chemicals and fuels. Ceria (CeO_2) catalyzes this reaction. But the conversion efficiency of CeO_2 is enhanced when the byproduct water in the reaction medium is separated by employing trapping agents like 2-cyanopyridine (2-CP). In this work, the influence of morphology of CeO_2 on the direct synthesis of DMC in presence of 2-CP is reported. CeO_2 catalysts of cube, rod, spindle and irregular morphology (Ce - C, Ce - R, Ce - S and Ce - N, respectively) were prepared, characterized and studied as catalysts in the said reaction conducted in a batch mode. Among all, Ce - S shows superior catalytic performance with nearly 100 mol% of DMC selectivity. Catalytic activity correlates with the concentration of acid and base sites of *medium strength* as well as defect sites. Ce - S has an optimum number of these active sites and thereby shows superior catalytic performance.

Keywords. CO_2 utilization; dimethyl carbonate; ceria; acid-base catalysis; influence of morphology.

1. Introduction

Climate change due to increasing amount of carbon dioxide (CO_2) emissions into atmosphere has become a major issue, for which much attention is being paid globally to control these emissions by way of converting CO_2 into fuels or chemicals. The Paris Climate Conference-2015 (COP21) recommended to limit the global temperature increase to less than 2°C above the present level by 2100.[1] This would be possible only if substantial (40–70%) reduction in CO_2 emissions is achieved by different countries by 2050. CO_2 is a cheap, non-toxic, non-flammable and abundant C_1 feedstock.[2–4] An efficient catalyst is needed for its activation and utilization due to its high thermodynamic stability and kinetic inertness. Conversion of CO_2 to dimethyl carbonate (DMC) has attracted interest as DMC is a green reagent/solvent, a raw material for manufacturing electrolytes used in lithium ion batteries and a potential gasoline additive with an annual demand of about 30 million tons.[5] DMC is a precursor in the synthesis of polycarbonates and isocyanates.[6,7] The traditional methods for DMC synthesis (phosgenation and oxidative carbonylation of methanol) are unsecure. Among several eco-friendly routes, its direct synthesis from methanol and CO_2 is atom-efficient and attractive.[8,9] Zirconia and ceria-based catalysts were most effective for this reaction.[5,10–14] However, the direct synthesis is low yielding and equilibrium limited. Removal of water co-generated in the reaction using traps is necessary to overcome those limitations. Recently, we reported the application of calcined zirconium phenylphosphonate phosphite as a catalyst for the direct synthesis of DMC.[15] Molecular sieve (3A) was used as a water trap. Methanol conversion of 31.8 mol% with DMC yield of 2.35 g/g-catalyst was achieved. In recent times, the research interest on the direct synthesis of DMC is mainly focused on ceria (CeO_2)-based catalysts due to their excellent activity as catalyst and catalyst support.[16–21] Wang *et al.*,[14] reported morphology control of CeO_2 nanocrystals on the direct synthesis of DMC. A synergism among the exposed (111) plane, defect sites, and acid-base sites was proposed to be crucial for getting high DMC formation. Spindle-shaped CeO_2 showed the highest DMC yield followed by nano-rods, nano-cubes and nano-octahedrons. Spindle-shaped CeO_2 enabled DMC yield of 1.382 mmol/g catalyst (reaction conditions: methanol amount = 15 mL, CO_2 = 5 MPa, reaction temperature = 140°C, reaction time = 2 h, catalyst weight = 0.1 g). DMC forms an azeotrope with methanol at atmospheric pressure, which demands distinct separation steps through extractive

*For correspondence

distillation, liquid–liquid extraction, evaporation, *etc*. In order to overcome such technical hurdles, a process which provides complete conversion of methanol to DMC is desired.

Honda *et al.*,[22] reported, for the first time, that CeO_2 along with benzonitrile as water trapping agent promotes the DMC yield even at CO_2 pressures as low as 0.1 MPa. The yields of DMC based on methanol and CO_2 were as high as 47% and 70%, respectively. Later the same group[23] reported the use of 2-cyanopyridine (2-CP) instead of benzonitrile and obtained quantitative conversion of methanol and CO_2 with the yield of DMC being 94% (scheme 1). Recently, Wang *et al.*,[24] reported the influence of morphologies of CeO_2 with different crystal faces (1 1 0), (1 0 0) and (1 1 1) on the hydrolysis of 2-CP. CeO_2-rods with a crystal face of (1 1 0) exhibited better activity than CeO_2-cube (1 0 0) and CeO_2-octahedron (1 1 1). Their study did not include the spindle morphology studied in the present investigation. Recently, Asahi Kasei Chemicals Corp.[25] declared construction of a validation plant for dialkyl carbonates to produce diphenyl carbonate using their proprietary catalyst. In view of the industrial importance of DMC, it is of interest to know the factors governing the catalytic activity/selectivity of CeO_2 in the direct synthesis route using 2-CP as a dehydrating agent. In this study, CeO_2 catalysts of cube, rod, spindle and irregular shape morphology (Ce - C, Ce - R, Ce - S and Ce - N, respectively) are prepared, characterized and studied as catalysts in the said reaction conducted in a batch reactor. The influence of structure of CeO_2 on the catalytic conversion of CO_2 was investigated.

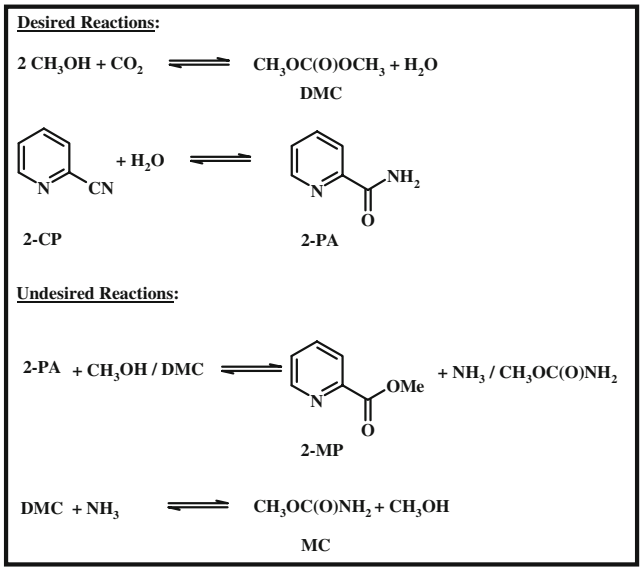

Scheme 1. Products in the direct synthesis of DMC from CO_2 and methanol in presence of 2-CP.

2. Experimental

2.1 *Catalyst preparation*

Ceria samples of different morphology were prepared by non-template hydrothermal synthesis methods as follows.[14,26]

2.1a *Ceria - spindles (Ce - S)*: A solution of 1.042 g of $Ce(NO_3)_3.6H_2O$ and 0.384 g of urea dissolved in 80 mL of distilled water was taken in a 100 mL Teflon-lined stainless-steel autoclave. The reactor was mounted in a rotating hydrothermal synthesizer (Hiro Co., Japan) and heated at 120°C for 8 h (stirring speed = 30 rpm). The precipitate obtained was separated by filtration and washed with distilled water and ethanol several times. After drying at 80°C for a day, the product was calcined at 600°C for 5 h.

2.1b *Ceria - cubes (Ce - C)*: 1.736 g of $Ce(NO_3)_3.6H_2O$ and 19.2 g of NaOH were dissolved separately in 10 and 70 mL of distilled water, respectively. These two solutions were mixed while stirring for 15 min at 25°C to get a purple-colored slurry which was then transferred into a 100 mL Teflon-lined stainless autoclave. The reactor was mounted in a rotating hydrothermal synthesizer (Hiro Co., Japan) and heated at 180°C for 24 h (stirring speed = 30 rpm). The precipitate obtained was separated by filtration and washed with distilled water and ethanol several times (until the pH of washing was neutral). After drying at 80°C for 1 day, the product was calcined at 600°C for 5 h.

2.1c *Ceria - rods (Ce - R)*: This sample was prepared following the same procedure as that of Ce - C except that the synthesis temperature was 100°C instead of 180°C.

2.1d *CeO_2– irregular morphology (Ce - N)*: For comparison, CeO_2 with irregular morphology (Ce - N) was also prepared. In a typical synthesis, 6.31 g of $Ce(NO_3)_3.6H_2O$ was dissolved in 180 mL of distilled water and transferred into a triple neck, glass, round-bottom flask fitted with water-cooled condenser and placed in an oil bath. The temperature of the oil bath was maintained at 80°C. In next step, 0.1 M aqueous NaOH solution was added into it drop-wise for 1 h with constant stirring till the pH was 10. Stirring was continued for another 3 h. It was then cooled to 25°C. The precipitate formed was separated by filtration and washed several times with distilled water until the pH of washings was 7. The solid obtained was dried at 80°C for 1 day and calcined at 600°C for 5 h.

2.2 *Characterization techniques*

The X-ray powder diffraction (XRD) patterns of the CeO_2 samples were recorded on a Philips X'pert Pro diffractometer using Cu-K_α radiation and a proportional counter detector. The diffraction patterns were recorded in the 2θ range of 10–90° at a scan rate of 4°/min. The step size in the measurements was 0.02°. High resolution transmission electron microscopic (HRTEM) images of the samples were collected on a FEI Technai-F30 instrument with a 300 kV field emission gun. FT-Raman spectra were recorded on a Horiba JY LabRaman HR 800 Micro Raman spectrometer with 632.8 nm wavelength generated by a He-Ne laser. Specific surface area (S_{BET}) of the samples was determined from the nitrogen adsorption measurements carried out at −196°C using a Quadrasorb SI automated surface area and pore size analyzer (Quanta Chrome Instrument). Before N_2 adsorption, the samples were evacuated at 200°C. S_{BET} was determined from the linear part of the BET equation ($p/p^\circ = 0.05$–0.31). The pore size distribution was calculated with the Barrett–Joyner–Halenda (BJH) method. Acidity and basicity of the catalysts were determined by a temperature-programmed desorption (TPD) technique using ammonia and carbon dioxide as probe molecules, respectively (Micromeritics Auto Chem 2910 instrument). About 0.1 g of the catalyst sample was activated at 200°C under a He gas flow (40 mL/min). The sample was cooled to 50°C and NH_3 (or CO_2) was adsorbed at a rate of 40 mL/min for 30 min. Then the temperature was raised to 100°C followed by purging with a He gas to remove the physisorbed probe molecule. After the stabilization of base line, desorption of probe molecules was followed in the temperature range 100–900°C at a ramp rate of 10°C/min. The TPD plot was deconvoluted and the amounts of acid/base sites of different strength were determined.

2.3 *Reaction procedure and product analysis*

Catalytic reactions were conducted in a 100 mL stainless-steel Parr pressure reactor. In a typical reaction, 3.2 g of methanol (100 mmol), 5.2 g of 2-CP (50 mmol) and 0.1 g of ceria catalyst were taken in the reactor which was then pressurized with CO_2 to 5 MPa. The temperature of the reactor was raised to a specific value (120–160°C) and the reaction was conducted for a known period of time (1–6 h) while stirring at a speed of 600 rpm. At the end of the reaction, the reactor was cooled to 25°C and the unreacted CO_2 was vented out. Then, 30 mL of ethanol and 0.2 g of nonan-1-ol were added to the liquid portion as a solvent and internal standard, respectively. Further, the mixture was stirred for 10 min to dissolve the solid 2-picolinamide (2-PA) completely in the liquid portion. The catalyst was separated out of the liquid portion by centrifugation followed by filtration. The liquid product was analyzed and quantified with a Varian 3400 gas chromatograph (GC) equipped with a flame ionization detector and CP-SIL5CB column (60 m long and 0.32 mm i.d.). Standard mixtures of methanol, DMC, 2-CP, 2-PA, 2-methyl picolinate (2-MP) and methyl carbamate (MC) were prepared, calibration plots were drawn and response factors of the reactants and products were determined. These were then used in quantifying the products. The following are the formulae used to describe conversion and product selectivity.

$$\%\ \text{MeOH conversion} = \frac{\text{mmol of MeOH consumed}}{\text{mmol MeOH taken}} \times 100$$

$$\%\ 2-\text{CP conversion} = \frac{\text{mmol of } 2-\text{CP consumed}}{\text{mmol of } 2-\text{CP taken}} \times 100$$

$$\%\ \text{DMC yield} = \frac{\text{mmol of DMC formed}}{(\text{mmol of MeOH taken}/2)} \times 100$$

$$\%\ 2-\text{PA yield} = \frac{\text{mmol of } 2-\text{PA formed}}{\text{mmol of } 2-\text{CP taken}} \times 100$$

$$\%\ \text{DMC selectivity} = \frac{\text{mmol of DMC formed}}{(\text{mmol of MeOH consumed}/2)} \times 100$$

$$\%\ 2-\text{PA selectivity} = \frac{\text{mmol of } 2-\text{PA formed}}{\text{mmol of } 2-\text{CP consumed}} \times 100$$

$$\%\ \text{MC selectivity} = \frac{\text{mmol of MC formed}}{\text{mmol of MeOH consumed}} \times 100$$

$$\%\ \text{MP selectivity} = \frac{\text{mmol of MP formed}}{\text{mmol of MeOH consumed}} \times 100 \quad \text{(based on MeOH)}$$

$$\%\ \text{MP selectivity} = \frac{\text{mmol of MP formed}}{\text{mmol of } 2-\text{CP consumed}} \times 100 \quad \text{(based on } 2-\text{CP)}$$

$$\text{MeOH mass balance} = \frac{\begin{pmatrix}\text{mmol of unreacted MeOH}\\ +2\text{ x mmol of DMC formed}\\ +\text{mmol of MC formed}\\ +\text{ mmol of MP formed}\end{pmatrix}}{\text{mmol of MeOH taken}} \times 100$$

$$2-\text{CP mass balance} = \frac{\begin{pmatrix}\text{mmol of unreacted } 2-\text{CP}\\ +\text{mmol of } 2-\text{PA formed}\\ +\text{mmol of MP formed}\end{pmatrix}}{\text{mmol of } 2-\text{CP taken}} \times 100$$

3. Results and Discussion

3.1 *Catalyst characterization*

XRD analysis showed characteristic peaks at 28.6, 33.1, 47.6, 56.6, 59.2, 69.6, 76.8, 79.3 and 88.6°, which could be indexed to CeO_2 with a cubic fluorite structure (unit cell parameter: a = 0.540 nm; space group of $Fm3^{-}m$; figure 1). The average crystallite size (determined from the full width at half maximum) and crystallinity (determined from the intensity of XRD peaks) of CeO_2 samples decreased in the order: Ce - C >Ce - S >Ce - N >Ce - R (table 1). HRTEM revealed that CeO_2 sample with a cubic morphology (Ce - C) contains particles of 20–140 nm size (figure 2a). Inter planar spacing (d-spacing) of 0.273 nm confirmed the exposed (100) planes in the cubic sample. A few exposed (111) planes were also traced (figure 2b). Ceria nano rods (Ce - R) have a diameter of 6.8 ± 1 nm and length of 50–100 nm (figure 2c). They contained exposed (111) and (200) planes with d-spacing of 0.311 and 0.270 nm, respectively (figure 2d). Ceria-spindles (Ce - S) were large in dimension. They had a length of 3–12 μm and width of 0.8–2.5 μm. The ends of the spindles were sharp and edges were curved indicating the existence of defect sites (figure 2e). They had exposed (111) planes (figure 2f). Ceria with irregular morphology (Ce - N) had a particle size in the range 10–16 nm (Supplementary Information, figure S1).

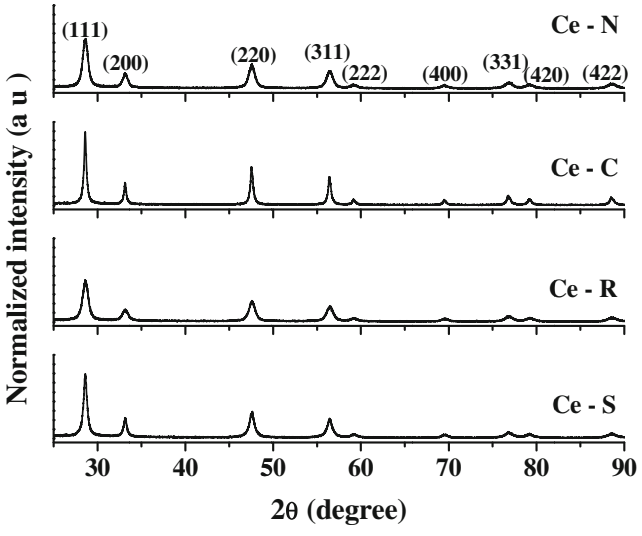

Figure 1. XRD patterns of CeO_2 with different morphologies.

FT-Raman spectrum showed an intense band at 463 cm^{-1} attributable to the F_{2g} mode of ceria fluorite phase and weak bands at 250, 600 and 1179 cm^{-1} corresponding to second-order transverse acoustic mode ($2T_A$), defect-induced mode and longitudinal optical mode, respectively (figure 3).[27,28] The intensity of the defects peak (at 600 cm^{-1}) was small due to its weaker sensitivity to visible Raman spectroscopy. The concentration of the defect sites (ratio of the area of Raman band due to defect-induced mode to the band due to the F_{2g} mode) was determined and found that Ce - S sample has higher amount of defect sites (1.1%) than Ce - N (0.8%), Ce - R (0.5%) and Ce - C (0.2%). The specific surface area (S_{BET}) of CeO_2 samples decreased in order: Ce - R (105 m^2/g) >Ce - N (77 m^2/g) >Ce - C (43 m^2/g) >Ce - S (36 m^2/g). This variation is in near agreement with that expected from their particle sizes.

NH_3-TPD showed three overlapping desorption peaks with peak maximum at 150–200°C, 320–360°C and 430–570°C, respectively (figure 4). While the first peak corresponded to weak Lewis acid sites, the second and third peaks are attributed to medium and strong acid sites. CO_2-TPD also exhibited three overlapping peaks at 150–160°C, 310–330°C and 480–550°C (figure 4) attributable to weak, medium and strong basic sites, respectively. The total acidity of the catalysts decreased in the order: Ce - C (454 μmol/g) >Ce - N (423 μmol/g) >Ce - S (285 μmol/g) >Ce - R (252 μmol/g) and basicity in the order: Ce - N (90 μmol/g) >Ce - S (85 μmol/g) >Ce - R (83 μmol/g) >Ce - C (65 μmol/g) (table 1). While Ce - C contained more amount of strong acid and base sites, the other samples contained a large amount of medium acid and base sites. The amount of strong acid sites was nearly the same for Ce - R, Ce - S and Ce - N. But the amount of strong basic sites was lower for Ce - R and Ce - S than for Ce - N and Ce - C. The concentration of medium acid and base sites decreased in the order: Ce - N >Ce - S >Ce - R >Ce - C. It should, however, be noted that the position of the desorption peak of medium and strong acid/base sites shifted to higher temperature as the morphology changed from cubes to rods to irregular shape to spindles. Thus, ceria with spindle morphology contained medium and strong acid/base sites of higher strength

Table 1. Textural, acid-base and catalytic properties of CeO_2 with different morphologies.

Sample	S_{BET} (m^2/g)	Average crystallite size (nm, XRD)	Particle size (μm; HRTEM)	Acidity (μmol/g; NH_3-TPD)[a]			Basicity (μmol/g; CO_2-TPD)[a]		
				Weak	Medium	Strong	Weak	Medium	Strong
Ce-N	77	12.0	–	106	240	77	16	51	23
Ce-C	43	23.7	0.02–0.14	85	128	241	12	25	28
Ce-R	105	11.2	0.05–0.1 × 0.007 ± 0.001	42	138	72	23	47	13
Ce-S	36	17.6	3–12 × 0.8–2.5	23	189	73	18	53	14

[a]Weak (<200°C), medium (200–400°C) and strong (>400°C).

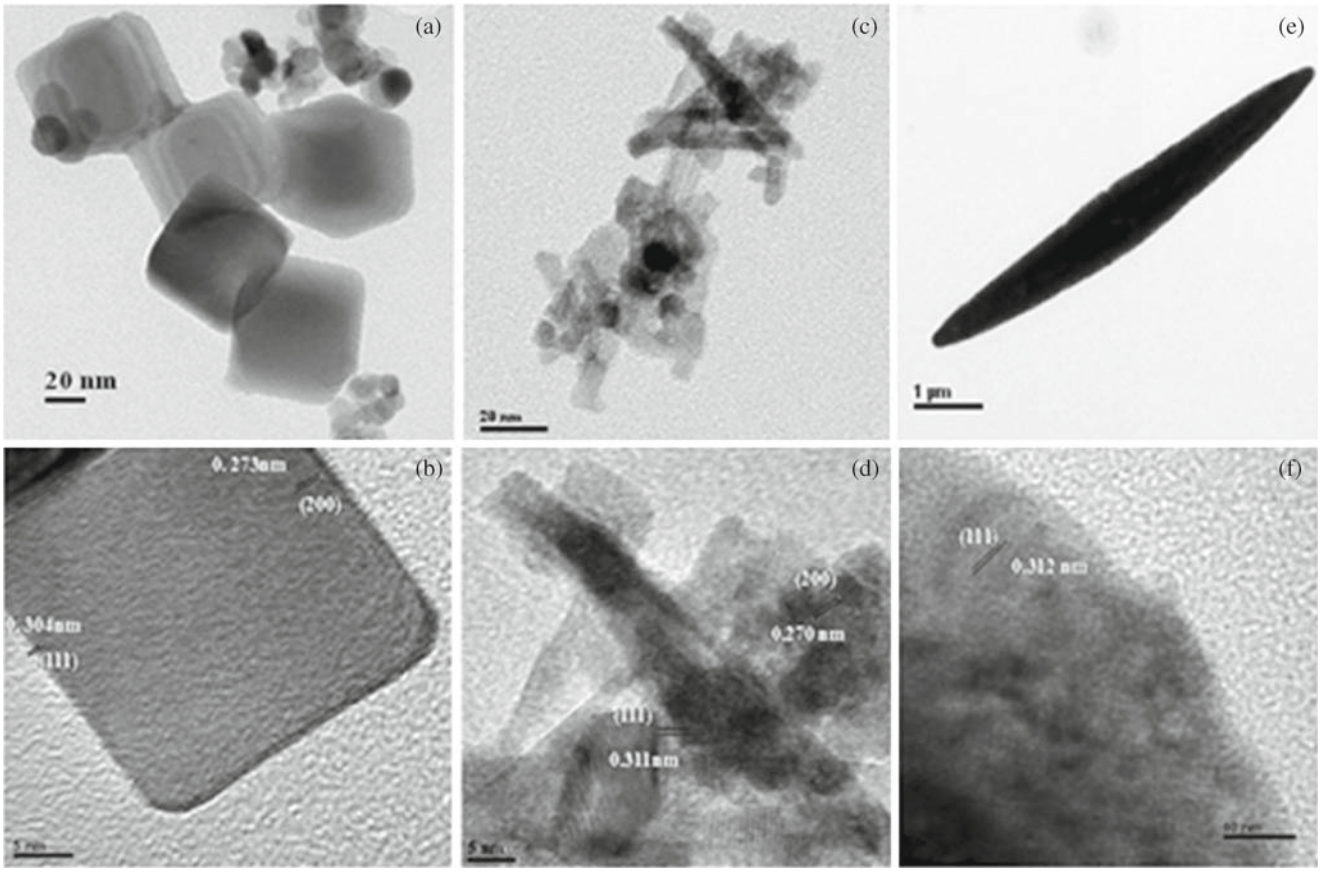

Figure 2. HRTEM images of CeO_2 samples: (a & b) Ce - C, (c & d) Ce - R and (e & f) Ce - S.

than those of rods, cubes and irregular morphology (figure 4).

3.2 *Catalytic Activity*

Controlled experiments (at 150°C for 2 h with CO_2 of 5 MPa) revealed that the reaction of methanol with CO_2 producing DMC (in presence of 2-CP as a dehydrating agent) did not occur without a CeO_2 catalyst. In agreement with the findings of others, the morphology of CeO_2 had a marked effect on the catalytic activity. The activity of ceria samples (methanol conversion) decreased in the order: Ce - S >Ce - N >Ce - R >Ce - C (table 2). Methanol and 2-CP conversions were 63.0 mol% over Ce - S catalyst and DMC and 2-PA formed with 97 mol% selectivity (table 2). With other catalysts, the yield of DMC was lower (≤35.4 mol%), and 2-methylpicolinate (2-MP) and methyl carbamate (MC) were detected in more amount (≥6.8 and 1.4 mol%, respectively). When the amount of the catalyst was raised from 0.1 to 0.3 g while keeping the other conditions the same, a quantitative conversion of methanol was observed over Ce - S. The influence of morphology of CeO_2 on product distribution (in mmol) and mass balance (liquid product) is reported in table 3. While the mass balance was 100% with Ce - S, it was

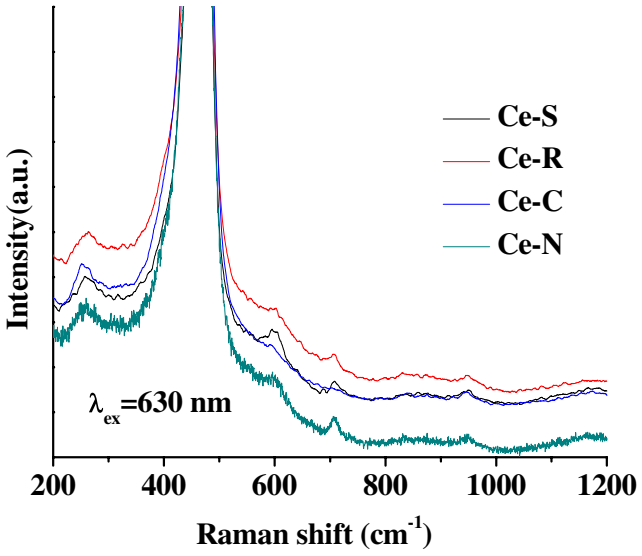

Figure 3. FT-Raman spectra of CeO_2 samples of different morphologies.

only 91% with Ce - R and Ce - C and 86% with Ce - N catalysts. Conversion of 2-CP was higher than the conversion of methanol. This suggests that a part of 2-CP got decomposed. Such decomposition was less for Ce - S than for other CeO_2 catalysts. Gas analysis pointed out that a part of DMC decomposed into dimethyl ether over Ce - R, Ce - C and Ce - N. This was not the case with Ce - S catalyst. In other words, the present study reveals that ceria sample of spindle morphology is highly active and selective.

Figure 5 demonstrates the influence of reaction temperature and reaction time on methanol conversion and DMC yield over Ce - S catalyst. Conversion of methanol increased with temperature and remained unaltered above 150°C. The yield of DMC reached a maximum at 150°C and above that, it decreased. This behavior is due to decomposition of DMC above 150°C. Methanol conversion and DMC yield increased with reaction time and remained constant after 3 h. The initial rate of the reaction over ceria-spindles was found to be 10.6×10^{-3} mmol.sec^{-1}. This reaction is exothermic in nature ($\Delta H = -27.90$ kJ.mol^{-1}).[29] Hence, higher temperature is unfavourable. However, to prevent poisoning of the surface active sites with CO_2, 2-CP and by-product water, and also to activate CO_2 for the reaction to occur on the solid surface, a temperature of about 150°C seems optimum.

Methanol conversion and DMC yield increased with increasing amount of medium type acid as well as base sites (figure 6). Deviation from linearity is perhaps due to difference in the strengths of acid/base sites of different ceria catalysts. The desorption occurred at higher temperature for Ce - S than for the other catalysts indicating that the strength of acid/base sites is higher for Ce - S. While the earlier report by Wang *et al.*, disclosed that the catalytic activity depends on acidity and

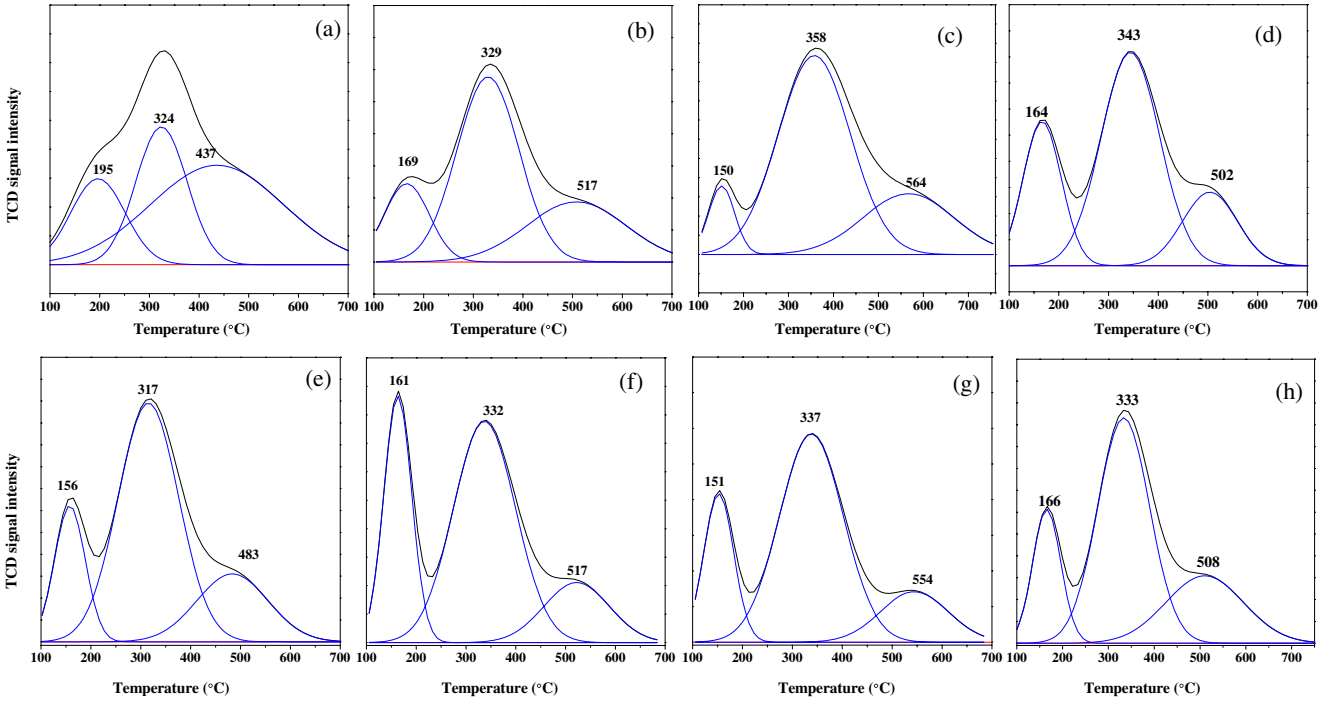

Figure 4. NH_3-TPD (top) and CO_2-TPD (bottom) profiles of Ce - C (a & e), Ce - R (b & f), Ce - S (c & g) and Ce - N (d & h).

Table 2. Catalytic activity data CeO_2 of different morphologies for the direct synthesis of DMC

Catalyst	Conversion (mol%)		Yield (mol%)		Product selectivity (mol%; based on methanol)			Product selectivity (%; based on 2-CP)	
	Methanol	2-CP	DMC	2-PA	DMC	MC	2-MP	2-PA	2-MP
Ce-N	51.2	64.6	31.6	44.0	61.7	2.1	6.8	68.1	10.8
Ce-C	37.3	49.6	31.4	33.2	84.2	1.4	9.4	66.9	14.1
Ce-R	50.0	61.8	35.4	45.4	70.8	2.2	7.0	73.5	11.3
Ce-S	63.0	63.0	61.0	60.8	97.0	1.2	2.9	96.5	5.4

Reaction conditions: methanol = 3.2 g (100 mmol), 2-cyanopyridine (2-CP) = 5.2 g (50 mmol), CO_2 pressure = 5 MPa, catalyst = 0.1 g, reaction temperature = 150°C, reaction time = 2 h.

Table 3. Influence of ceria morphology on the product distribution and mass balance in the direct synthesis of DMC.

Catalyst	Product distribution (mmol)						Mass balance (%)	
	Methanol	2-CP	DMC	2-PA	MC	2-MP	Based on methanol	Based on 2-CP
Ce-N	48.8	17.7	15.8	22.0	1.1	3.5	85	86
Ce- C	62.7	25.2	15.7	16.6	0.5	3.5	98	91
Ce-R	50.0	19.1	17.7	22.7	1.1	3.5	90	91
Ce-S	40.4	18.5	30.5	30.4	0.7	1.7	104	101

Reaction conditions: Methanol = 3.2 g (100 mmol), 2-cyanopyridine = 5.2 g (50 mmol), CO_2 pressure = 5 MPa, catalyst = 0.1 g, reaction temperature = 150°C, reaction time = 2 h.

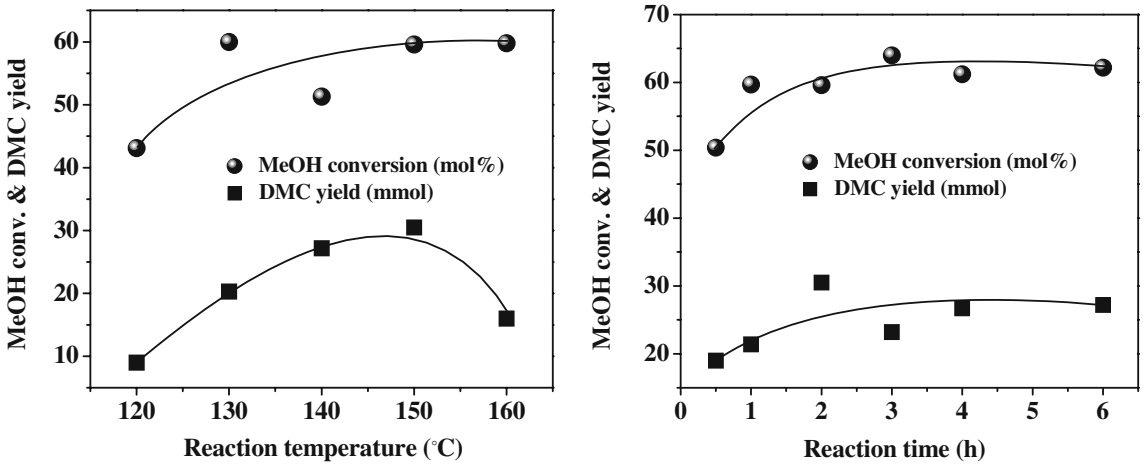

Figure 5. Influence of, (left) reaction temperature, and (right) reaction time on DMC yield over Ce - S catalyst. Reaction conditions: methanol = 3.2 g, 2-CP = 5.2 g, CO_2 pressure = 5 MPa and catalyst = 0.1 g for, (a) t = 2 h, and for (b) T = 150°C.

basicity, the present study narrows it down specifically to medium type acid/base site.

While the basic sites are responsible for formation of methoxide ions, the acid sites assist in generating CH_3^+ ions from methanol. A perfect tuning of the acidic and basic sites is crucial for achieving 100% DMC selectivity. Ce - S has a right balance of these active sites and thereby shows higher conversion and DMC selectivity. A tentative mechanism for DMC over CeO_2 catalysts is presented in figure 7.

Methanol conversion (mol%) should be equal to 2-CP conversion. But, an excess amount of 2-CP got converted on Ce - N, Ce - R and Ce - C catalysts (table 2). This is due to a large percentage of strong acid sites present on those catalysts that decompose a part of 2-CP taken in the reaction. DMC yield correlated with the concentration of defect sites as well. The defect sites act as a source to activate CO_2. The high defect morphology (Ce - S in the present study) adsorbs more CO_2, which is further activated by the base sites

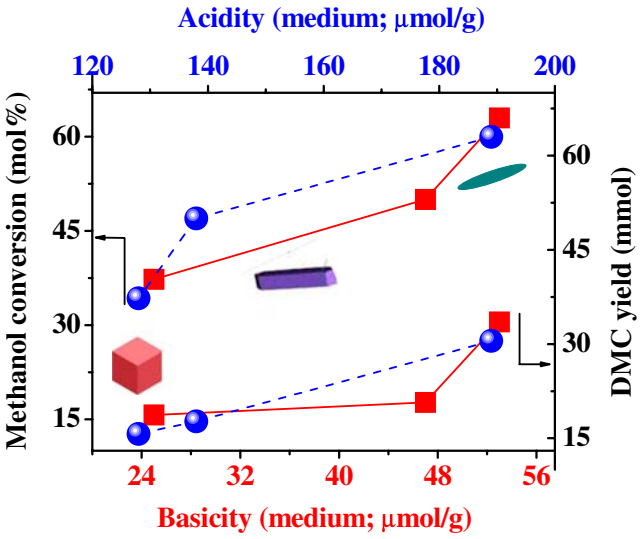

Figure 6. Correlation between catalytic activity (methanol conversion and DMC yield) and density of acid/base sites of *medium* strength of CeO_2 catalysts. Reaction conditions: same as in table 2.

of medium strength present on the catalyst. In addition to acid/base and defect sites, exposed facets may also control the catalytic activity.

The most stable surface (111) is the active surface for this reaction. Ceria sample with spindle morphology has a large amount of these exposed facets. Thus, acid-base sites of *medium strength*, defect sites, exposed (111) facet and morphology control the catalytic activity and selectivity of CeO_2 in the direct synthesis of DMC from methanol and CO_2.

4. Conclusions

The direct synthesis of DMC from methanol and CO_2 in presence of 2-CP (dehydrating/water trapping agent) was studied over CeO_2 samples of different morphologies. CeO_2 with spindle morphology was found superior to rods, cubes and irregular shape morphologies. Quantitative conversion of methanol with nearly 100 mol% selectivity for DMC was obtained over Ce - S catalyst. Methanol conversion and DMC yield correlates with the concentration of acid/base sites of medium strength, exposed (111) facets and defect sites. The highest catalytic activity of Ce - S is attributed to its spindle morphology having a right balance of medium acid-base sites and defect centers. While this study confirms some of the earlier findings, it points out

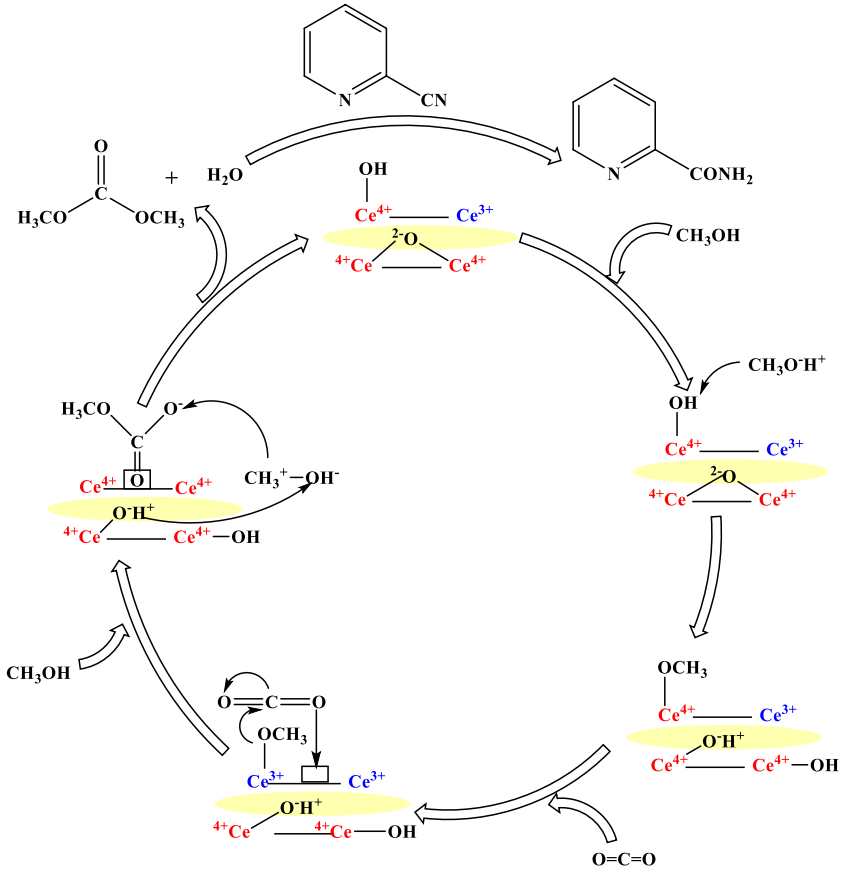

Figure 7. Possible mechanism for DMC synthesis from methanol and CO_2 over CeO_2 catalysts.

the importance of acid/base sites of medium strength in the catalytic reaction.

Supplementary Information (SI)

HRTEM images of Ce - N sample and catalytic activity data of Ce - S as a function of reaction temperature and reaction time are available as supporting information on the website of Journal of Chemical Sciences at www.ias.ac.in/chemsci.

Acknowledgements

P.U. acknowledges CSIR, New Delhi for the fellowship. This work forms a part of the Project "TapCoal (CSC 0102)" sponsored by CSIR.

References

1. http://www.cop21.gouv.fr/en/why-2c/ (accessed on 01 January 2016)
2. Arresta M 2010 In *Carbon dioxide as a chemical feedstock* (Weinheim: Wiley-VcH Verlag)
3. Unnikrishnan P and Srinivas D 2015 In *Industrial catalysis and separations: Innovations for process intensification* (NJ, USA: Apple Academic)
4. Sakakura T, Choi J C and Yasuda H 2007 *Chem. Rev.* **107** 2365
5. Honda M, Tamura M, Nakagawa Y and Tomishige K 2014 *Catal. Sci. Technol.* **4** 2830
6. Tundo P and Selva M 2002 *Acc. Chem. Res.* **35** 706
7. Fukuoka S, Fukawa I, Tojo M, Oonishi K, Hachiya H, Aminaka M, Hasegawa K and Komiya K 2010 *Catal. Surv. Asia* **14** 146
8. Unnikrishnan P and Srinivas D 2015 *J. Mol. Catal. A: Chem.* **398** 42
9. Huang S, Yan B, Wang S and Ma X 2015 *Chem. Soc. Rev.* **44** 3079
10. Eta V, Mäki-Arvela P, Wärnå J, Salmi T, Mikkola J P and Murzin D Y 2011 *Appl. Catal. A: Gen.* **404** 39
11. Tomishige K and Kunimori K 2002 *Appl. Catal. A: Gen.* **237** 103
12. Jung K T and Bell A T 2001 *J. Catal.* **204** 339
13. Ikeda Y, Asadullha M, Fujimoto K and Tomishige K 2001 *J. Phys. Chem. B* **105** 10653
14. Wang S, Zhao L, Wang W, Zhao Y, Zhang G, Ma X and Gong J 2013 *Nanoscale* **5** 5582
15. Unnikrishnan P, Varhadi P and Srinivas D 2013 *RSC Adv.* **3** 23993
16. Vinodkumar T, Naga Durgasri D, Swamy M and Reddy B M 2015 *J. Chem. Sci.* **127** 1145
17. Naga Durgasri D, Vinodkumar T and Reddy B M 2014 *J. Chem. Sci.* **126** 429
18. Dutta G, Gupta A, Waghmare U V and Hegde M S 2011 *J. Chem. Sci.* **123** 509
19. Sanjaykumar S R, Mukri B D, Patil S, Madras G and Hegde M S 2011 *J. Chem. Sci.* **123** 47
20. Gayen A, Baidya T, Ramesh G S, Srihari R and Hegde M S 2006 *J. Chem. Sci.* **118** 47
21. Mishra B G, Ranga Rao G and Poongodi B 2003 *Proc. Ind. Acad. Sci. (J. Chem. Sci.)* **115** 561
22. Honda M, Kuno S, Sonehara S, Fujimoto K-i, Suzuki K, Nakagawa Y and Tomishige K 2011 *Chem. Cat. Chem.* **3** 365
23. Honda M, Tamura M, Nakagawa Y, Sonehara S, Suzuki K, Fujimoto K and Tomishige K 2013 *Chem. Sus. Chem.* **6** 1341
24. Wang S P, Zhou J J, Zhao S Y, Zhao Y J and Ma X B 2015 *Chin. Chem. Lett.* **26** 1096
25. http://www.asahi-kasei.co.jp/asahi/en/news/2014/e150119.html (accessed on 16 April 2015)
26. Fan T, Zhang L X, Jiu H F, Sun Y X, Liu G D, Sun Y Y and Su Q L 2010 *Micro Nano Lett.* **5** 230
27. Nakajima A, Yoshihara A and Ishigame M 1994 *Phys. Rev. B* **50** 297
28. Wu Z, Li M, Howe J, Meyer H M and Overbury S H 2010 *Langmuir* **26** 16595
29. Eta V, Maki-Arvela P, Leino A R, Kordas K, Salmi T, Murzin D Y and Mikkola J P 2010 *Ind. Eng. Chem. Res.* **49** 9609